WARWICK
THE UNIVERSITY OF WARWICK

Original citation:
Zhang, Binjia, Xie, Fengwei, Shamshina, Julia L., Rogers, Robin D., McNally, Tony, Wang, David K., Halley, Peter J, Truss, Rowan W, Zhao, Si-ming and Chen, Ling. (2017) Facile preparation of starch-based electroconductive films with ionic liquid. ACS Sustainable Chemistry & Engineering.

Permanent WRAP URL:
http://wrap.warwick.ac.uk/88417

warwick.ac.uk/lib-publications

Facile preparation of starch-based electroconductive films with ionic liquid

Binjia Zhang[a,b,c], Fengwei Xie[,c], Julia L. Shamshina[d,e], Robin D. Rogers[e], Tony McNally[f],*

*David K. Wang[g], Peter J. Halley[c], Rowan W. Truss[c], Siming Zhao[b], Ling Chen[**,a]*

[a] Guangdong Province Key Laboratory for Green Processing of Natural Products and Product Safety, South China University of Technology, 381 Wushan Road, Guangzhou, Guangdong 510640, China

[b] Key Laboratory of Environment Correlative Dietology (Ministry of Education), College of Food Science and Technology, Huazhong Agricultural University, 1 Shizishan Street, Wuhan, Hubei 430070, China

[c] School of Chemical Engineering, The University of Queensland, Brisbane, Queensland 4072, Australia

[d] 525 Solutions, Inc., 720 2nd Street, Tuscaloosa, Alabama 35401, United States

[e] Department of Chemistry, McGill University, 801 Sherbrooke Street West, Montreal, Quebec H3A 0B8, Canada

[f] International Institute for Nanocomposites Manufacturing (IINM), WMG, University of Warwick, Coventry CV4 7AL, United Kingdom

[g] School of Chemical and Biomolecular Engineering, The University of Sydney, Darlington, NSW 2006, Australia

[*] *Corresponding Author. Email: f.xie@uq.edu.au, fwhsieh@gmail.com (F. Xie)*

[**] *Corresponding Author. Email: felchen@scut.edu.cn (L. Chen)*

KEYWORDS: *Starch-based materials; Ionic liquid; 1-Ethyl-3-methylimidazolium acetate; Plasticizer; Energy-saving processing; Electroconductive films*

1
2
3
4
5
6
7
8
9
10
11
12
13
14
15
16
17
18
19
20
21
22
23
24
25
26
27
28
29
30
31
32
33
34
35
36
37
38
39
40
41
42
43
44
45
46
47
48
49
50
51
52
53
54
55
56
57
58
59
60

ABSTRACT: Here, we discovered that starch could be straightforwardly processed into optically-transparent electroconductive films, by compression molding at a relatively mild temperature (55 °C or 65 °C), much lower than those commonly used in biopolymer melt processing (typically over 150 °C). Such significantly-reduced processing temperature was achieved with the use of an ionic liquid plasticizer, 1-ethyl-3-methylimidazolium acetate ($[C_2mim][OAc]$). A higher $[C_2mim][OAc]$ content, lower processing temperature (55 °C), and/or higher relative humidity (RH) (75%) during the sample post-processing conditioning, suppressed the crystallinity of the processed material. The original A-type crystalline structure of starch was eliminated, although small amounts of B-type and V-type crystals were formed subsequently. The starch crystallinity could be linked to the mechanical properties of the films. Moreover, the processing destroyed the original lamellar structure of starch, and the amorphous starch processed with $[C_2mim][OAc]$/water could aggregate on the nanoscale. The films displayed excellent electrical conductivity ($> 10^{-3}$ S/cm), which was higher with a lower processing temperature (55 °C) and a higher conditioning RH (75%). The incorporation of $[C_2mim][OAc]$ reduced the thermal decomposition temperature of starch by 30 °K, while the formulation and processing conditions did not affect the film thermal stability.

INTRODUCTION

Nowadays, bio- or "green" materials from renewable resources are increasingly selected for reasons of environmental sustainability and carbon impact.[1] Biopolymers can be referred to as polymers directly from biomass, a natural, abundant and underutilized source of renewable feedstocks, which principally are cellulose, hemicellulose, chitin, starch, and lignin. Biopolymers are not only widely available and sustainable, but also can be biodegradable and biocompatible, and thus have several economic and environmental advantages. Moreover, the societal recognition and expectation for environmentally-friendly products create a demand for technically advantageous materials that can replace petroleum-derived plastics.

The application of biopolymers heavily relies on their processability into usable forms. However, the processing of biopolymers is somewhat challenging due to the strong intermolecular hydrogen bonding in their native forms,[2] and the processing conditions usually depend on the identity of the biopolymer. Traditionally, for the film formation, biopolymers have been mostly processed by solution methods (casting), based on a film-forming solution (more rare, dispersion) where biopolymers are first solubilized into a liquid phase. Organic solvent systems, capable of disruption of hydrogen bonding (*e.g.*, DMF, DMAc), are utilized, which, after casting of the film, are removed (usually by drying at a higher temperature).[3] However, these methods are much less efficient and less suitable for industrial-scale production due to significant use of corrosive solvent systems. In another method of film casting, ionic liquids (ILs, salts that melt below 100 ^{o}C) are used in place of VOCs, to solubilize biopolymers. Thus, we have recently shown that reproducible, strong, and versatile cellulose[4-5] or chitin films,[6] made from either

biopolymer alone or combined with other polymer(s), can be prepared through the dissolution of biopolymer in 1-ethyl-3-methylimidazolium ($[C_2mim][OAc]$) ionic liquid (IL) followed by the casting of films and washing out the solvent. Films prepared using this methodology can be prepared with the controlled composition, thickness, surface properties, flexibility, and transparency.

While the melt processing of biopolymers has also been practiced,[7-9] high processing temperature, high viscosity, and easy thermal decomposition during processing remains to be challenges.[3, 10-11] With chemical modification, biopolymers can be converted into soluble forms (*e.g.,* cellulose acetate) or derivatives that are more processable (*e.g.*, hydroxypropyl starch). Nevertheless, such conversion not only increases the costs but also modifies the inherent properties of the biopolymers. Besides, for promoting environmental sustainability and reducing carbon impact, people have put more emphasis on material production technologies requiring less energy input.

To this end, plasticizers that are effective in disrupting the native hydrogen-bonding network of biopolymers could provide solutions for the easier and "greener" treatment of biopolymers. Starch, a polysaccharide found in plants such as maize (corn), potato, cassava, wheat, and rice, represents a typical model with a naturally complex structure involving strong intermolecular hydrogen bonding. In the native form of granules (<1 μm~100 μm), starch has a multi-level hierarchical structure, which is based on two major biomacromolecules, amylose (mainly linear) and amylopectin (hyper-branched) (~nm). Nevertheless, between the granule and molecular levels, there are alternating amorphous and semicrystalline shells (growth rings) (100~400 nm), with the latter shell being stacked crystalline and amorphous lamellae (periodicity) (9~10 nm).[12-15] Therefore,

it is important to understand how the complex structure of starch can be altered to achieve the desired plasticized forms.

With a plasticizer and elevated temperature, a process known as "gelatinization" (with abundant plasticizer content) or "melting" (with limited plasticizer content) occurs, resulting in a disruption of the 3D structure of native starch. If preferential conditions are reached, this process can lead to a homogeneous amorphous material known as "thermoplastic starch (TPS)" or "plasticized starch," which is essential in the production of some starch-based materials.[3, 10-11, 16] For the dissolution of starch, in particular, water is the most commonly-used solvent, although the process does not take place at room temperature resulting only in starch swelling, and high temperatures are needed for its complete dissolution;[17-18] yet, phase separation often occurs. Such phase separation (*i.e.*, heterogeneous conditions) makes aqueous systems to be unfavorable for starch processing. Substances such as polyols (*e.g.*, glycerol, glycol, sorbitol), compounds containing nitrogen (*e.g.*, urea, ammonium derived, amines), and citric acid have been reported to be effective for the plasticization of starch,[3, 10] but not for its dissolution. Other well-known solvents for starch is dimethyl sulfoxide (DMSO),[19] often with the addition of salts such as calcium chloride ($CaCl_2$),[20] urea/alkali (NaOH) aqueous solution,[21] concentrated mineral and organic acids,[22] ethylene diamine,[23] pyridine,[24] or *N,N*-dimethylacetamide (DMAc)/lithium chloride (LiCl) system.[25-26] These solvents are corrosive, toxic, often hydrolyze polymer decreasing its molecular weight (MW), many are unsuitable for biomedical applications, often volatile, and usually difficult to recycle.

A plasticizer for starch should preferably be thermally-stable and non-volatile both during thermal processing and in post-processing stages, be ineffective in enhancing

starch macromolecular degradation, be non-toxic to humans and the environment, and be able to promote starch-based materials with enhanced performance and new capabilities. Unfortunately, commonly used plasticizers do not yet have all the desired attributes and thus finding alternative and better plasticizers for starch is of interest. By avoiding many of the reactive chemicals and facilitating a physical dissolution process, ionic liquids (ILs) overcome the disadvantages of "conventional" dissolution/plasticization practices.[27]

ILs that contain a strongly basic, hydrogen bond accepting anion (*e.g.*, carboxylates or halides) have the ability to wholly or partially disrupt the intermolecular hydrogen bonding present in biopolymeric networks. As a result, ILs are demonstrated to either fully dissolve or plasticize many biopolymers such as starch,[28-32] cellulose,[33-34] chitin/chitosan,[35-37] silk fibroin,[38-40] lignin,[41] zein protein,[28] and wool keratin.[42] As such, these ILs can be used as excellent media for polysaccharide plasticization and modification resulting in the development of advanced biomaterials, such as ionically conducting polymers or solid polymer electrolytes.[43-50] For example, 1-ethyl-3-methylimidazolium acetate ([C$_2$mim][OAc]) has desirable properties, *e.g.*, low toxicity (LD$_{50}$ > 2000 mg·kg^{-1}), low corrosiveness, low melting point (< -20 °C), low viscosity (10 mPa·s at 80 °C), and favorable biodegradability.[51]

For the processing of polysaccharides with ILs, solution methods were predominantly involved in previous studies. Sankri *et al.*[52] and Leroy *et al.*[53] have done pioneering work using an IL 1-butyl-3-methylimidazolium chloride ([C$_4$mim][Cl]) as a new plasticizer for melt processing of starch-based materials, which demonstrated improved plasticization, electrical conductivity, and hydrophobicity. Our previous work[54] has shown that [C$_2$mim][OAc] has a significant plasticization effect on starch, including high-amylose

starch, prepared via a thermal compression molding process, and can reduce the crystallinity and make the amorphous phase more mobile leading to desirable properties for some specific applications (*e.g.*, electrically-conductive materials). However, in these past efforts, a high temperature (up to 160 °C) and/or multiple processing steps were required to fabricate starch-based films. Such high-temperature conditions make it difficult to incorporate thermally-sensitive ingredients (such as bioactive ingredients and enzymes) into starch-based materials.

In contrast to the previous work, this paper reports a facile and energy-saving process to create starch-based electrically-conductive films. In this research, the one-step compression molding process required only a mild temperature (55 °C or 65 °C) to transform native starch into a transparent material with electrical conductivity. Furthermore, we revealed that the structure and properties of the resultant material could be easily tailored by the formulation and processing conditions.

EXPERIMENTAL SECTION

Materials

A chemically-unmodified regular maize starch (RMS) was supplied by New Zealand Starch Ltd. (Onehunga, Auckland, New Zealand) with the product name "Avon Maize Starch". This starch has an amylose content of 24.4%.[55] The original moisture content (MC) of this starch was 13.6 wt.% as measured by a Satorius Moisture Analyser (Model MA30, Sartorius Weighing Technology GmbH, Weender Landstraβe 94-108, 37075, Goettingen, Germany). Milli-Q water was used in all instances. [C$_2$mim][OAc] of ≥95wt% purity (with *ca.* 1200 ppm water content), produced by IoLiTec Ionic Liquids

Technologies GmbH (Salzstraβe 184, D-74076 Heilbronn, Germany) was also supplied by Chem-Supply Pty Ltd.

$[C_2mim][OAc]$-aqueous solutions: $[C_2mim][OAc]$ is a liquid completely miscible with water at room temperature.[56] In this work, 0.15:1 mol/mol $[C_2mim][OAc]$:water solution was prepared, where this mole ratio accounted for the MC of starch and the purity and MC of the IL.

Film preparation

Two formulations were used for the film preparation (see Table S1 and S2 in Support Information (SI)). 0.15:1 mol/mol $[C_2mim][OAc]$:water solution was added drop-wise to the starch, accompanied by careful blending using a mortar and pestle to ensure an even distribution of the liquid mixture in the starch. Then, the blended samples were hermetically sealed and stored in Ziploc® bags under ambient conditions (*ca*. 28 °C) for at least 4 h, before thermal compression molding. The storage allowed time for further equilibration of the samples. The blended sample was carefully and uniformly spread over the molding area with poly(tetrafluoroethylene) glass fabrics (Dotmar EPP Pty Ltd, Acacia Ridge, Qld, Australia) located between the starch and the mould. Then, compression molding was undertaken at a specific temperature (55 °C or 65 °C) under pressure (8 MPa) for 30 min. After opening the mold, an optically transparent sample (9 cm × 6 cm, thickness *ca.* 1.2 mm) could be retrieved. The films were conditioned at two different relative humidities (RH), 33% (over-saturated magnesium chloride solution) and 75% (over-saturated sodium chloride solution),[57] at room temperature in desiccators for 7 days before material characterizations. From the sample preparation to conditioning, no observation indicated that $[C_2mim][OAc]$ phased out of the starch films. This

suggested a strong binding between [C$_2$mim][OAc] and the starch. The MCs in the samples were subject to change during conditioning. After the conditioning, the thickness of all films was *ca*. 1 mm. Table 1 shows the compositions in mass and mole ratios after conditioning. The MCs were determined by weighing the samples before and after vacuum-oven drying at 100 °C for 48 h to remove all the moisture.

Table 1. Mass and mole ratios of different starch-[C$_2$mim][OAc] films

Sample	Mass ratio			Mole ratio of IL and water content relative to hydroxyl groups (−OH) in starch		
	Starch (dry basis)	[C$_2$mim][OAc]	water	Starch hydroxyl	[C$_2$mim][OAc]	water
IL18-T55-H33	99.36 ± 0.00	60 ± 0	28.59 ± 0.20	1 ± 0	0.18 ± 0.00	0.86 ± 0.01
IL18-T55-H75	99.36 ± 0.00	60 ± 0	55.06 ± 0.99	1 ± 0	0.18 ± 0.00	1.66 ± 0.03
IL18-T65-H33	99.36 ± 0.00	60 ± 0	28.54 ± 0.58	1 ± 0	0.18 ± 0.00	0.86 ± 0.02
IL18-T65-H75	99.36 ± 0.00	60 ± 0	54.78 ± 0.40	1 ± 0	0.18 ± 0.00	1.65 ± 0.01
IL21-T55-H33	86.40 ± 0.00	60 ± 0	29.44 ± 0.49	1 ± 0	0.21 ± 0.00	1.02 ± 0.02
IL21-T55-H75	86.40 ± 0.00	60 ± 0	53.72 ± 0.56	1 ± 0	0.21 ± 0.00	1.87 ± 0.02
IL21-T65-H33	86.40 ± 0.00	60 ± 0	30.11 ± 0.19	1 ± 0	0.21 ± 0.00	1.05 ± 0.01
IL21-T65-H75	86.40 ± 0.00	60 ± 0	53.95 ± 0.41	1 ± 0	0.21 ± 0.00	1.87 ± 0.01

In the following text, the plasticized starch samples are coded in the format of "IL18-T55-H33", where "IL18" denotes the IL content (0.18) in a mole ratio relative to starch hydroxyls (see SI Table S2), "T55" shows the temperature used for compression molding, and "H33" indicates the relative humidity (RH) for conditioning.

Characterization

Sample compositions. The MCs were determined gravimetrically. Namely, the samples were placed in a vacuum oven at 100 °C for 48 h, which allowed the removal of all the moisture. The samples were weighed before and after the oven drying to estimate the MCs. At least three replicates were used for determining the MC of each sample.

Scanning electron microscopy (SEM). The starch samples were cryo-ground in liquid nitrogen. The fractures were put on circular metal stubs previously covered with double-sided adhesive before platinum coating at 5 nm thickness using an Eiko Sputter Coater, under vacuum (7×10^{-3} bar). The morphology of the starch samples was examined using a scanning electron microscope (SEM, JEOL JSM-6460LA, Tokyo, Japan). An accelerating voltage of 5 kV and a spot size of 6 nm were used. A magnification of 1000× was used for all the images.

Powder X-ray diffraction (pXRD). The starch film samples (size *ca.* 2 cm × 2 cm) were placed in the sample holder of a X-ray powder diffractometer (D8 Advance, Bruker AXS Inc., Madison, WI, USA) equipped with a graphite monochromator, a copper target, and a scintillation counter detector. pXRD patterns were recorded for an angular range (2θ) of 4–40°, with a step size of 0.02° and a step rate of 0.5 s per step, and thus the scan time lasted for approximately 15 min. The radiation parameters were set at 40 kV and 30 mA, with a slit of 2 mm. Traces were processed using the Diffrac Plus Evaluation Package (Version 11.0, Bruker AXS Inc., Madison, WI, USA) to determine the X-ray diffractograms of the samples. The degree of crystallinity was calculated with the PeakFit software (Version 4.12, Systat Software, Inc., San Jose, CA, USA) following the method by Lopez-Rubio, et al. [58] Eq. (1):

$$X_c = \frac{\sum_{i=1}^{n} A_{ci}}{A_t}$$

(1)

where A_{ci} is the area under each crystalline peak with index i, and A_t is the total area (both amorphous background and crystalline peaks) under the diffractogram.

The V-type crystallinity (single-helical amylose structure) was quantitatively estimated based on the total crystalline peak areas at 7.5°, 13°, and 20° following the method provided in reference.[59]

Attenuated total reflectance Fourier-transform infrared (ATR-FTIR) spectroscopy. The ATR-FTIR spectra of different starch samples were recorded using a Nicolet 5700 FTIR spectrometer (Thermo Electron Corporation, Madison, WI, USA) equipped with a Nicolet Smart Orbit attenuated total reflectance (ATR) accessory incorporating a diamond internal reflection element. For each spectrum, 64 scans were recorded over the range of 4000–600 cm^{-1} at RT (about 22 °C) at a resolution of 4 cm^{-1}, co-added and Fourier-transformed. The background spectrum was recorded on air and subtracted from the sample spectrum. ATR-FTIR spectra were baseline-corrected and deconvoluted using PeakFit (v4.12). The ratio of band intensities at 995 cm^{-1} and 1022 cm^{-1} was used for analyzing the film molecular rearrangement.

Synchrotron small-angle X-ray scattering (SAXS). SAXS analysis was carried out on the SAXS/WAXS beamline (flux, 10^{13} photons/s) at the Australian Synchrotron (Clayton, Vic., Australia), at a wavelength λ = 1.47 Å. The 2D scattering patterns were collected using a Pilatus 1M camera (active area 169 × 179 mm; and pixel size 172 ×

172 μm). The scatterBrain software was used to acquire the one-dimensional (1D) data from the 2D scattering pattern; and the data in the angular range of $0.0015 < q < 0.15$ Å^{-1} was used as the SAXS pattern, in which $q = 4\pi\sin\theta/\lambda$ (where 2θ is the scattering angle and λ is the wavelength of the X-ray source).[60-61] All data were background subtracted and normalized. The starch-based films were placed on a multi-well stage provided by the Australian Synchrotron, and then the SAXS data recorded for an acquisition time of 1 s.

For the SAXS patterns, the inflection data centered at around 0.007 Å^{-1} were fitted using a unified model Eq. (2):[62]

$$I(q) = G\exp\left(-\frac{R_g^2 q^2}{3}\right) + C\left(\frac{\left[erf\left(\frac{qR_g}{\sqrt{6}}\right)\right]^3}{q}\right)^{\alpha} \qquad (2)$$

In this equation, G is the pre-factor of the Guinier function corresponding to a radius R_g; and C and α are the pre-factor and the exponent of the power-law function, respectively.

Tensile testing. Tensile tests were performed with an Instron® 5543 universal testing machine (Instron Pty Ltd, Bayswater, Vic., Australia) with a 500N load cell on dumbbell-shaped specimens cut from the sheets with a constant deformation rate of 10 mm/min at room temperature. The specimens corresponded to Type 4 of the Australian Standard AS 1683:11 (ISO 37:1994), and the testing section of each specimen was 12 mm in length and 2 mm in width. Young's modulus (E), tensile strength (σ_t), and elongation at break (ε_b) were determined by the Instron® software, from at least 7 specimens for each of the plasticized starch samples.

Thermogravimetric analysis (TGA). A Mettler Toledo TGA/DSC1 machine (Mettler-Toledo Ltd., Port Melbourne, Vic., Australia) was used with 40 μL aluminum crucibles with a cap with a pinhole for thermogravimetric analysis (TGA) under nitrogen. This equipment was calibrated using the melting points of Au, Zn and In standards (1064 °C, 419.5 °C, and 155.6 °C, respectively). A sample mass of about 5 mg was used for each run. The samples were heated from 25 °C to 550 °C and measured in the dynamic heating regime, using a constant heating ramp of 3 K/min.

Electrical conductivity. An alternating current (AC) impedance spectroscopy method was used to measure the proton conductivity of each film in a conductivity cell. The resistance of the films was probed by a frequency response analyzer (FRA, CompactStat, Ivium Technologies B. V., The Netherlands) with an oscillating voltage of 20 mV over a frequency range of 1 MHz − 1 Hz. The conductivity of starch films was tested at room temperature (*ca.* 26 °C) at a RH of 33% or 75% using a Model 740 Membrane Testing System (MTS, Scribner Associates, Inc., Southern Pines, NC, USA). A 15 min equilibration time was used at each RH before the measurement. The conductivity (σ, S/cm) of the film samples was calculated using Eq. (3):

$$\sigma = \frac{l}{A \times R}$$

(3)

where l (cm) is the film thickness, A (cm^2) the film area, and R (Ω) the film resistance.

RESULTS AND DISCUSSION

Sample compositions

Table 1 shows the composition (in mass ratios and mole ratios) of different [C$_2$mim][OAc]-plasticized starch-based films. The MC of the film was adjusted using conditioning at a certain RH in a humidity chamber (see Experimental). At the same RH, a higher MC could result from a higher [C$_2$mim][OAc] content in the film (see SI Table S1 and S2 for the original formulations for sample preparation). These phenomena could be ascribed to the strong hydrophilicity of [C$_2$mim][OAc], which had a stronger affinity to water than to starch hydroxyls, and played the major role in the moisture absorption of the films from the environment.[63] As the electrical conductivity of starch-[C$_2$mim][OAc] films is mainly related to the moisture and IL contents in the films, RH can potentially tailor the electrical conductivity of starch-[C$_2$mim][OAc] films.[64]

Visual appearance

Immediately after compression molding and before conditioning, different [C$_2$mim][OAc]-plasticized starch-based films were placed on top of a paper sheet printed with The University of Queensland (UQ) logos to indicate their optical transparency. All starch-[C$_2$mim][OAc] films displayed high transparency, showing the proper plasticization of starch by [C$_2$mim][OAc]. IL21-T65 was observed having the highest transparency, while IL18-T55 was least transparent. These results were as expected as a higher [C$_2$mim][OAc] (lower starch content) and/or a higher processing temperature could facilitate interactions between [C$_2$mim][OAc] and starch molecules, *i.e.*, a stronger plasticization effect. Abundant plasticization could disrupt the sophisticated granule structure of native starch, leading to the higher transparency of the film.

Surface morphology

Figure 1 collects the SEM images of the normal and fracture surfaces of starch-[C$_2$mim][OAc] films under either 33% or 75% RHs. IL18-T55-H33/75 were observed still containing the apparent starch granule shapes that were not destroyed during processing. With a reduced starch content in the formulation, IL21-T55-H33/75 also displayed such granule shapes on its surfaces. It has been reported that even after gelatinization in abundant water, there are still some granule shells that are not destroyed. These granule shells could be similar to "ghosts",[65] which are formed due to the physical crosslinking of polysaccharide chains within swollen granules.[66]
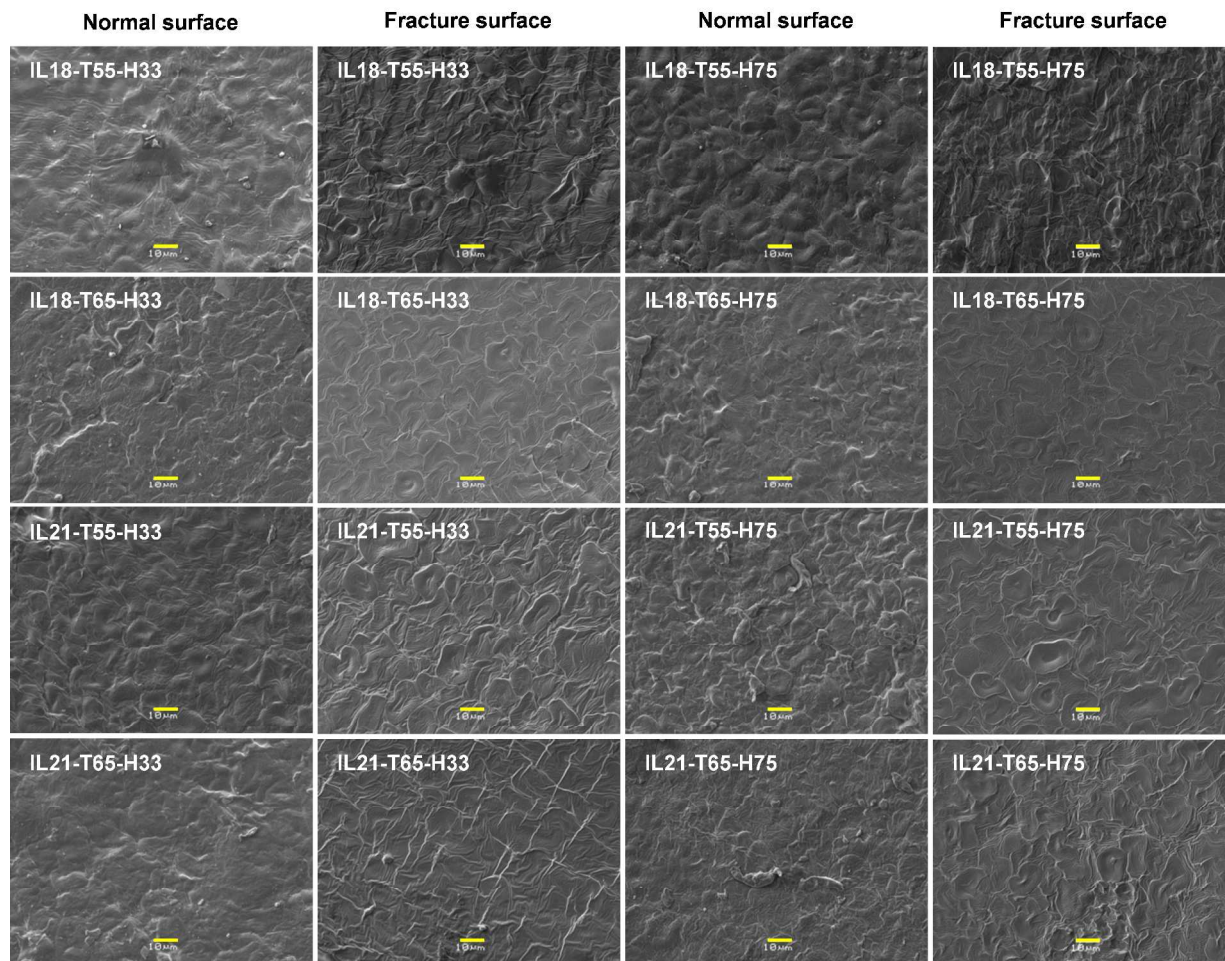
Figure 1. SEM images of normal and fracture surfaces of starch-[C$_2$mim][OAc] films. The spot size was 6 nm. The scale bar (yellow) indicates 10 μm.

With a higher processing temperature (IL18-T65-H33/75 and IL21-T65-H33/75), these remaining granules became much less apparent, and the surface morphologies became more homogeneous and smooth. These results suggested that at a higher temperature, the aqueous IL was more effective in the disruption of the native starch structure and the disentanglement of starch molecules. Nonetheless, the two starch contents used did not result in any significant difference in morphology.

Crystalline structure

Powder X-ray diffraction (pXRD) provides an elucidation of the long-range molecular order in the polymer. There are three polymorphic crystalline structures of starch, termed A, B or V-type, and the types of crystallinity can be unambiguously distinguished by inspecting the characteristic X-ray diffraction patterns.[14, 67] This is important as each type of the starch crystalline structures interacts differently with water molecules. Normally, in the crystalline structure of native starch, A-type and B-type polymorphs are found; both are left-handed, six-fold structures. However, the A-type polymorph is arranged as H-bonded parallel-stranded double helices (one double helix at the corner and another at the center of the unit cell) packed in a B2-monoclinic space group;[67] such close-packed arrangement allows for capture of only four water molecules in the unit cell. Water thus cannot be removed from A-type starch without a complete destruction of its crystalline structure. The double helices of B-polymorph are packed into a hexagonal unit cell, $P6_1$ space group,[67] and thus the arrangement is more open allowing for a presence of larger number of water molecules, located in a central channel surrounded by six double helices. Here as many as thirty-six water molecules are located in the unit cell between the six double helices,[68] creating a "column" of water surrounded by the hexagonal network. Finally, V-type polymorph is arranged into a single, left-handed helix, where the hydroxyl groups of the glucose units all lie nearly in the plane of the ring, resulting in a larger hydrophobic central cavity.

Figure 2 shows the pXRD pattern for the native starch and different starch-[C_2mim][OAc] films. Native RMS showed the typical A-type pattern, with strong reflections at 2θ of about 15° and 23° and an unresolved doublet at 2θ of 17° and 18°,

with a few weak peaks at 2θ of about 26°, 30°, and 33°.[55, 69] For the plasticized samples,

the doublet at 2θ of 17° and 18° disappeared, suggesting a complete loss of the A-type

pattern. Besides, the plasticized samples displayed the weak V_H-type pattern as shown by

sharp peaks at 2θ of 7°, 13°, and 20°,[59] and the modest B-type pattern as indicated by

strong reflections at 2θ of 5°, 17°, 22° and 24°.[55, 69] The V_H-type crystalline structure is

commonly observed in processed starch, which is caused by the rapid recrystallization of

single-helical structures of amylose during cooling after processing.[59] While the

plasticized RMS had both (newly-formed) V_H-type and B-type crystalline structures, the

crystallinity was low as indicated by the reduced XRD intensities. In particular, IL21-

T55-H75 and IL21-T65-H75 were predominantly amorphous. Based on these results, the

combination of high $[C_2mim][OAc]$ and moisture contents could make the starch chains

too mobile to arrange into crystals during the processing and conditioning.
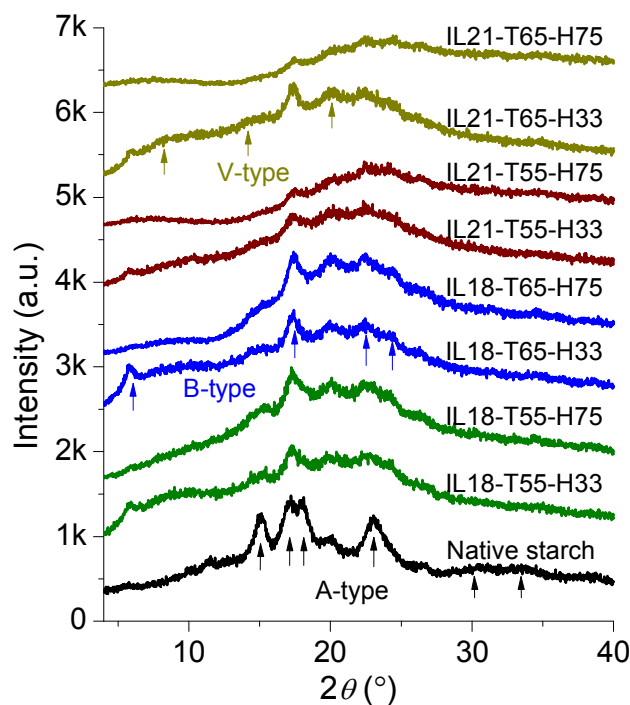
Figure 2. pXRD patterns for native starch and starch-[C$_2$mim][OAc] films.

Table 2 lists the XRD parameters for the changes in crystalline structure. The total crystallinity (X_c) of the native starch was 38.62%, including 37.53% for the A-type crystalline structure and the rest 1.09% for V-type. IL21-T55-H33 had reduced X_c of just 4.66% (containing 3.99% for B-type and 0.68% for V-type). With a higher processing temperature, IL21-T65-H33 had higher total X_c and higher X_c for both the B- and V-type crystalline structures. These results suggested a higher temperature could allow stronger interactions between starch and [C$_2$mim][OAc], which facilitated the rearrangements of starch molecules to form new crystals. However, at 75% RH, these rearrangements might be restricted to some degree, as seen from IL21-55-75 and IL21-65-75 with reduced X_c values. With both high [C$_2$mim][OAc] and MCs, the interactions of these liquids with

starch hydroxyls could dominate, and thus the interactions between starch molecules were inhibited.

Table 2. Parameters for crystalline structure of native starch and starch-$[C_2mim][OAc]$ films.

Sample	X_c (%) measured by XRD [a]				ATR-FTIR band intensity ratio
	Total	A-type	B-type	V-type	$R_{995/1022}$
Native starch	38.62	37.53	–	1.09	–
IL18-T55-H33	6.63	–	6.01	0.61	2.297 ± 0.026
IL18-T55-H75	6.23	–	5.64	0.59	2.066 ± 0.018
IL18-T65-H33	7.07	–	6.24	0.83	2.282 ± 0.020
IL18-T65-H75	6.53	–	5.77	0.76	2.054 ± 0.022
IL21-T55-H33	4.66	–	3.99	0.68	1.940 ± 0.015
IL21-T55-H75	4.04	–	3.49	0.55	1.829 ± 0.023
IL21-T65-H33	5.27	–	4.24	1.03	2.002 ± 0.028
IL21-T65-H75	4.60	–	3.79	0.81	1.876 ± 0.019

[a] XRD values are within $\pm 1\%$

ATR-FTIR results can also reflect the change in starch orders. Specifically, the absorption band intensity at 1022 cm^{-1} relates to the amorphous parts, while that at 995 cm^{-1} corresponds to the hydrogen bonding and the regularity resulting from molecular rearrangements. Therefore, the band intensity between 995 cm^{-1} and 1022 cm^{-1} ($R_{995/1022}$) can be used to study the recrystallization of starch-based materials.[70] Figure 3 shows the ATR-FTIR spectra for the native starch and starch-$[C_2mim][OAc]$ films, with

the $R_{995/1022}$ values shown in Table 2. It can be seen that $R_{995/1022}$ was increased with processing temperature and starch content, suggesting a higher degree of molecular rearrangements. A higher RH reduced $R_{995/1022}$ ratio, which meant a higher MC did not favor the molecular rearrangements. All these results were consistent with the XRD analysis.
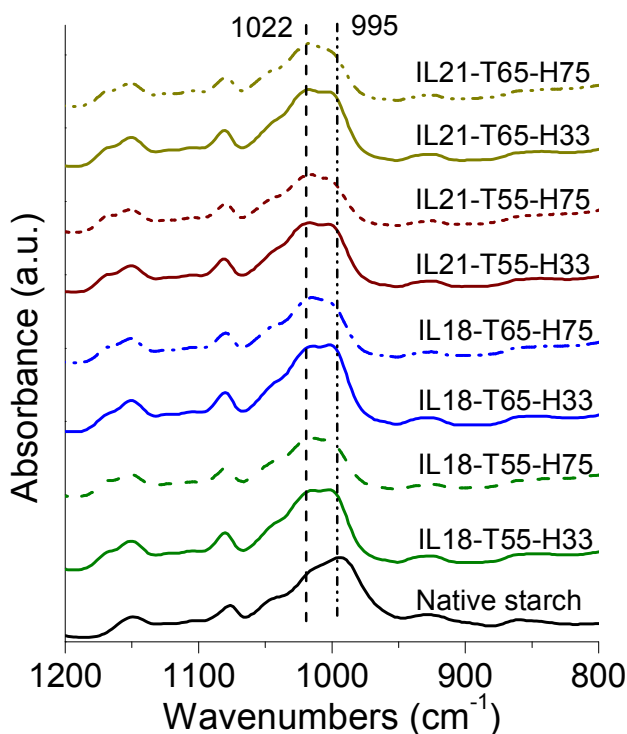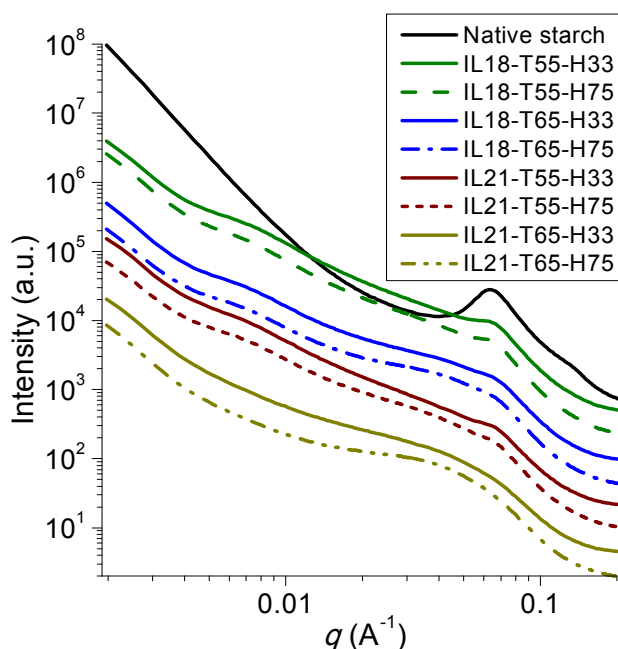

Figure 3. FTIR spectra for native starch and starch-[C$_2$mim][OAc] films.

Nano-structural features

Figure 4 presents the synchrotron-SAXS patterns for the native starch and starch-[C$_2$mim][OAc] films. As expected, the native starch had a characteristic SAXS peak at

ca. 0.06 Å^{-1}, ascribed to its native semicrystalline lamellae.[71] IL18-T55-H33 displayed a weaker lamellar peak than the native starch, and a new inflection at *ca.* 0.007 Å^{-1}. This inflection could be correlated to the Guinier scattering behavior, *i.e.*, a structure with a certain radius of gyration, R_g.[72] Here, this inflection could be attributed to the aggregates of starch chains (mainly amorphous) with [C$_2$mim][OAc]-water molecules on the nanoscale (R_g: *ca.* 60 nm) (see Table 3).

Figure 4. SAXS patterns for native starch and starch-[C$_2$mim][OAc] films.

Also can be seen in Figure 4 that a lower starch content and/or a higher processing temperature reduced the visibility of the lamellar peak. The other two inflections could be seen at *q* values lower than the lamellae peak position (*ca.* 0.007 Å^{-1} and 0.04 Å^{-1}). Regarding this, the increased [C$_2$mim][OAc] content and processing temperature

facilitated the disruption of starch semi-crystalline lamellae, from which the out-phasing

of starch molecules was enhanced. These starch molecules aggregated into not only the

aggregates with increased R_g but also new starch aggregates of a smaller size (R_g: *ca.*

10 nm). At a higher RH, the inflection at *ca.* 0.04 Å^{-1} became more apparent, indicating

the stronger feature of starch aggregates, presumably due to the increased content of

amorphous starch (indicated by the XRD results).

Table 3. Nanostructural parameters for native starch and starch-[C$_2$mim][OAc] films.

Sample	q (Å^{-1})	d_{Bragg} (nm)	R_{g} (nm)	α
Native starch	0.0629 ± 0.0000	9.99 ± 0.00	–	–
IL18-T55-H33	0.0610 ± 0.0000	10.30 ± 0.00	59.11 ± 1.17	1.97 ± 0.02
IL18-T55-T75	0.0610 ± 0.0000	10.30 ± 0.00	62.80 ± 1.47	1.96 ± 0.02
IL18-T65-T33	0.0610 ± 0.0000	10.30 ± 0.00	68.76 ± 2.33	1.75 ± 0.02
IL18-T65-T75	0.0610 ± 0.0000	10.30 ± 0.00	71.89 ± 3.02	1.69 ± 0.02
IL21-T55-H33	0.0616 ± 0.0008	10.20 ± 0.14	67.45 ± 1.53	1.86 ± 0.01
IL21-T55-H75	0.0610 ± 0.0000	10.30 ± 0.00	69.54 ± 2.07	1.77 ± 0.02
IL21-T65-H33	–	–	8.64 ± 0.08	2.60 ± 0.03
IL21-T65-T75	–	–	8.86 ± 0.05	2.78 ± 0.03

For IL21-T65-H33/75, no lamellar peak was observed as that for the native starch.

Instead, at that *q* range, a "shoulder" peak appeared at *ca.* 0.06 Å^{-1}. This shoulder

indicated a molecular organization (both amorphous and ordered starch) on the

nanoscale.[73] In other words, a concomitant reduction in starch content and an increase in

processing temperature prominently enhanced the plasticization of starch by [C$_2$mim][OAc] acting as flexible spacers (typically between the amylopectin branching points) in starch-based films.[74-75] This plasticization effect led to the alignment of amorphous starch and crystallites in a certain distribution range on the nanoscale. Again, the inflection at *ca.* 0.007 Å^{-1} (*i.e.*, the starch aggregates) disappeared, indicating an increase in the homogeneity of starch-[C$_2$mim][OAc] films (IL21-T65-H33/75).

Mechanical properties

Figure 5 shows the tensile properties of different starch-based films, tensile strength (σ_t), Young's modulus (*E*), and elongation at break (ε_b). All three factors, composition, temperature and relative humidity affected the mechanical properties. Generally, a larger amount of starch resulted in higher tensile strength of the films, *i.e.*, tensile for IL18 was greater than for IL21 films. Contrarily, but expectedly, elongation at break (also known as fracture strain) that represents the capability of a material to resist changes of shape without crack formation was greater with a higher amount of plasticizer ([C$_2$mim][OAc]-water). The composition affected Young's modulus to somewhat greater extent than it did for tensile and elongation at break, thus films with greater starch content a great increase in Young's modulus. Relative humidity had a larger effect on tensile strength and elongation at break than on Young's modulus, which was independent of humidity but affected by the amount of polymer in films. Both tensile strength and elongation were greater at a lower humidity. Finally, the samples processed at a higher temperature had greater tensile strength and elongation; again humidity was much stronger dependent on composition than on processing and conditioning conditions.
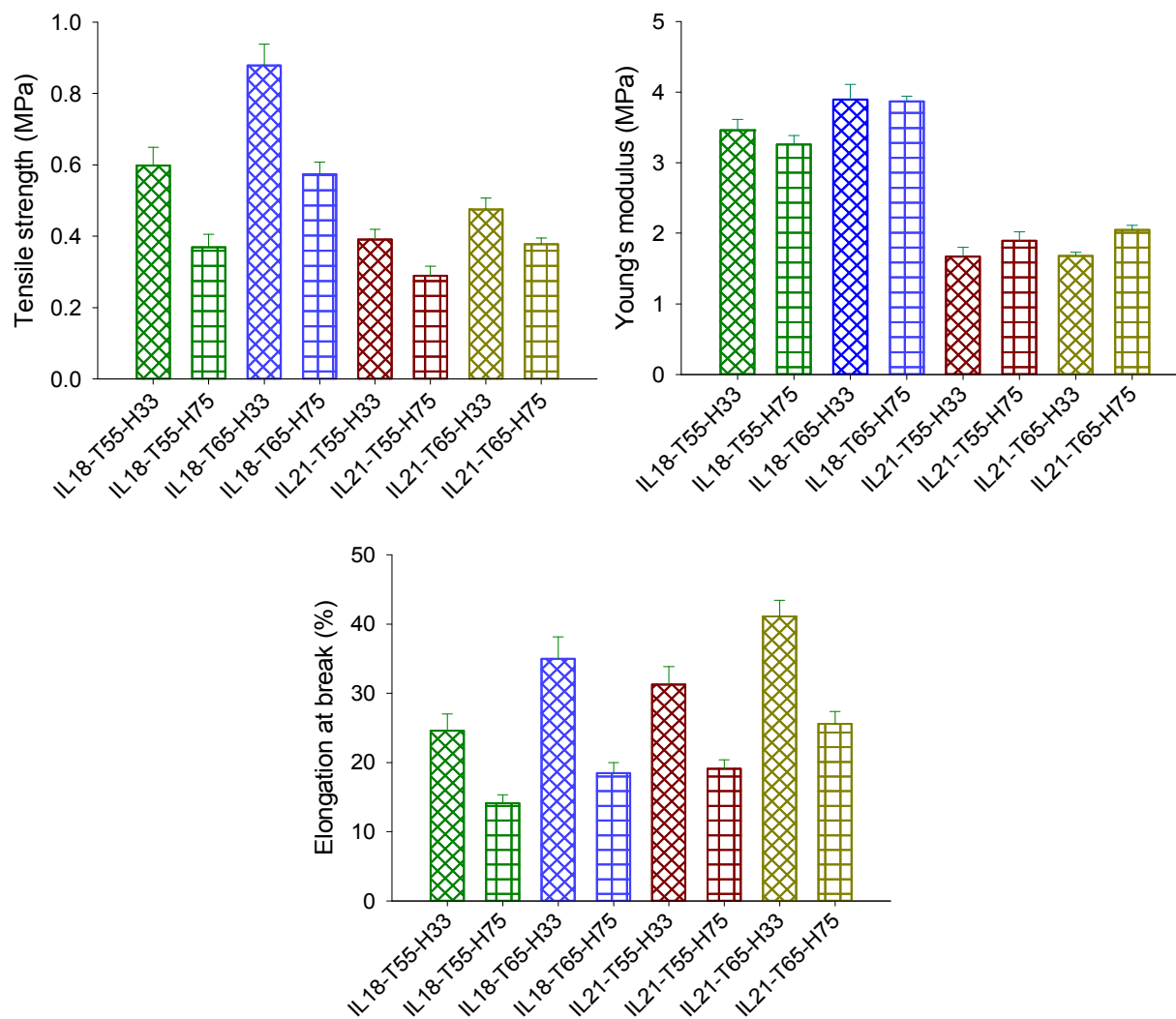
Figure 5. Tensile strength (σ_t), Young's modulus (E), and elongation at break (ε_b) of starch-[C$_2$mim][OAc] films.

A higher processing temperature facilitated plasticization by disrupting the original hydrogen bonding in the native starch allowing the formation of new crystals and molecular entanglements as indicated by the pXRD and SAXS results. These new structures could mechanically reinforce the materials.

Except for IL18-T55-H75 (whose crystallinity X_c was determined to be 6.23 %), the rest of the films follows the clearly pronounced trend: the higher crystallinity, the higher tensile strength. On the other hand, a higher starch content (lower [C$_2$mim][OAc] content) contributed to higher σ_t, and E and lower ε_b (except for the effect of RH on IL21-T55 and IL21-T65). These results were expected considering the plasticization effect of plasticizers ([C$_2$mim][OAc] and water). Both [C$_2$mim][OAc] and water could result in a partial disruption of hydrogen bonding between starch molecules, forming hydrogen bonds with –OH sites of starch. Besides, [C$_2$mim][OAc] and water could effectively increase the free volume of starch macromolecules, resulting in reduced strength and stiffness. Moreover, the plasticizers prevented macromolecular entanglement, resulting in less "connections" between the polymer chains, as demonstrated by higher ε_b. Regarding the opposite trend for IL21-T55-H33/75 and IL21-T65-H33/75 as affected by RH, it was proposed when the samples were well saturated by [C$_2$mim][OAc] and/or water, both the polymer elasticity and the structural effect of the plasticizers could contribute to lower E. Perhaps the strong interactions between [C$_2$mim][OAc] and water [63] might also influence E.

Also, compared with IL/glycerol-plasticized starch films prepared by a high temperature (e.g. 160 °C) melt processing,[76-78] the starch-[C$_2$mim][OAc] films here developed at mild temperatures had lower σ_t and E, but higher or comparative ε_b. This phenomenon could be mainly attributed to the lower starch content (higher IL-water content) in this work, which contributed to the reduced strength and stiffness and the weakened "connections" between the starch chains for the starch-IL films as discussed above.

Thermal stability

Figure 6 shows the TGA results for the pure IL, the native starch, and different starch-[C$_2$mim][OAc] films. It can be seen that pure [C$_2$mim][OAc] had a big derivative weight loss peak between about 160 °C and 275 °C, showing its thermal decomposition. This temperature range of TGA decomposition is exactly in agreement with a previous study which documented the lower thermal stability of acetate IL's than IL's containing other anions like [Cl$^-$].[79] Also, starting from about 75 °C, there was a slight weight loss immediately before the decomposition, which might be ascribed to the evaporation of impurities present in the starting materials (< 5%, mainly acetic acid, methylimidazole, and water).
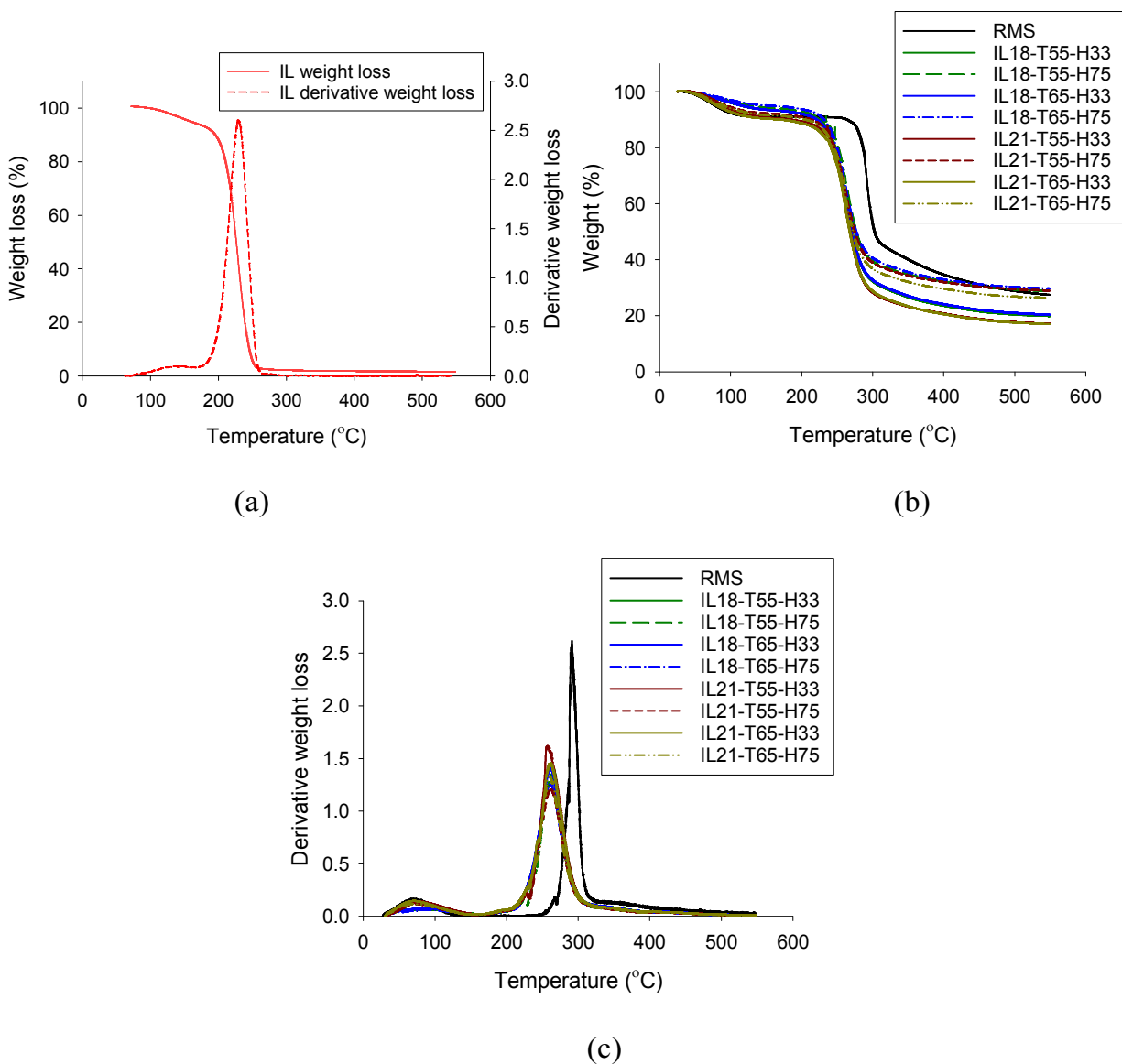
(a)

(b)

(c)

Figure 6. TGA results of the pure IL (a), and different starch-[C$_2$mim][OAc] films (b, weight loss; c, derivative weight loss).

For the native starch, there was a weight loss between *ca.* 40 °C and 140 °C, due to the evaporation of moisture in the starch. After that, the thermal decomposition of starch occurred between *ca.* 240 °C and 330 °C, which was in agreement with previous

studies.[80-81] This main peak could be specifically associated with the breakage of long chains of starch as well as the thermal oxidation of the glucose rings.[80]

All the processed starch-based films displayed a very similar thermal decomposition profile. The main decomposition spanned from 185 °C to 330 °C. As previous studies have shown that the thermal decomposition temperature of pure $[C_2mim][OAc]$ was from *ca.* 160 °C to 275 °C,[78] the peak for $[C_2mim][OAc]$ would be overlapped by the thermal decomposition peak of the native starch. The main decomposition (the maximum rate of weight loss, or derivative peak, at *ca.* 260 °C) occurred much earlier for the processed samples than for the native starch (derivative peak at *ca.* 290 °C). Thus, all starch-$[C_2mim][OAc]$ films had reduced thermal stability, which was in agreement with the previous studies.[54, 64, 78] No difference was observed for the different starch-based films, irrespective of $[C_2mim][OAc]$ or water content and RH. Water/$[C_2mim][OAc]$ should have already had reached the maximum interactions with the starch. Hence no effect could be seen regarding the thermal stability of the films.

Electrical conductivity

Electrical conductivity is an important characteristic of $[C_2mim][OAc]$-plasticized polymer films. Wang *et al.* [44] prepared starch-based films plasticized by 30 wt.% 1-allyl-3-methylimidazolium chloride ([Amim][Cl]), which had an electrical conductivity as high as $10^{-1.6}$ S/cm at 14.5 wt.% water content. Sankri *et al.*[52] showed that starch-based films plasticized by 30 wt.% 1-butyl-3-methylimidazolium chloride ([C₄mim][Cl]) had an electrical conductivity of $10^{-4.6}$ S/cm at 13 wt.% water content. Sankri *et al.*[52] proposed that the high electrical conductivity obtained by Wang *et al.*[44] may be explained by increased ion mobility due to the ion pair dissociation mechanism described by Zhang *et*

al. [33]. This ion pair dissociation might not be apparent for [Amim][Cl] resulting in more localized ions in the case of [Amim][Cl]-plasticized starch. Also, as the ion diffusivity and mobility mainly control the conductivity, the anion should be small with delocalized charge.

Figure 7 shows the electrical conductivity results for the different samples in this work. All the samples had good electrical conductivity ($>10^{-3}$ S/cm). In particular, IL21-T55-H33 and IL21-T55-H75 showed the highest electrical conductivity of 0.0055 and 0.0118 S/cm, respectively. Also, for the samples with the same starch content and conditioned at the same RH, a lower processing temperature (55 °C instead of 65 °C) could lead to a higher electrical conductivity. In these results, a higher processing temperature allowed [C$_2$mim][OAc] and water molecules to strongly interact with the starch, which might have reduced the extent of ion pair dissociation.

From Figure 7, a general trend could be identified that either an increase in RH or [C$_2$mim][OAc] content could increase the electrical conductivity, with the effect of RH being more significant. Wang, et al. [44] have indicated that increasing ion concentration by increasing the IL content could improve the conductance of plasticized starch films effectively, and similarly, a high water content can promote a better transference of the anions and cations in the films.
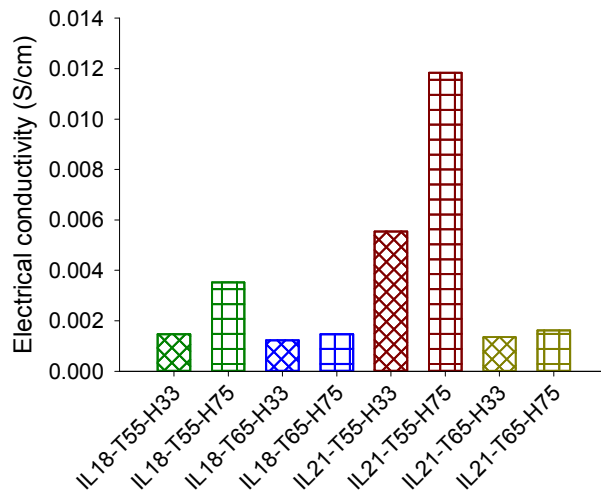
Figure 7. Electrical conductivity of starch-[C$_2$mim][OAc] films.

CONCLUSION

In this work, we demonstrate that starch can be processed into optically transparent films easily and rapidly by compression molding at mild temperatures (55 °C or 65 °C), which are much lower than the temperatures commonly used in the thermal melt processing of biopolymer (typically over 150 °C). This process was achieved with the use of an ionic liquid, [C$_2$mim][OAc], which was assisted by a high processing pressure (8 MPa) to disrupt the sophisticated and resistant granule structure of native starch. Moreover, the structure and properties of the resultant films could be tailored by starch content, compression molding temperature, and/or RH used for the sample post-processing conditioning.

With the pXRD analysis, it was found that the simple processing eliminated the original A-type crystalline structure of starch and the processed materials contained newly

formed crystals (predominantly B-type and some V-type). These new structures could contribute to enhanced mechanical properties (σ_t, E, and ε_b). Nonetheless, a higher [C$_2$mim][OAc] content, lower processing temperature (55 °C), and/or higher RH (75%) during conditioning reduced the crystallinity and even resulted in an amorphous material. Also, SAXS revealed that the processing could destroy the original lamellar structure of starch, and the plasticized starch tended to form a gel-like structure on the nanoscale in a coordinated fashion, which could be favored by increased processing temperature and conditioning RH. The starch-[C$_2$mim][OAc] films displayed excellent electrical conductivity ($>10^{-3}$ S/cm), which was higher with a lower processing temperature (55 °C) and a higher conditioning RH (75%). With the use of [C$_2$mim][OAc], the thermal stability of starch-based films was reduced by 30 °K but was independent of the formulation and processing conditions.

Our findings here could not only benefit the development of advanced biopolymer-based materials with tailored structure and properties such as electrical conductivity but also guide the evolution of material processing techniques for reducing energy consumption as well as enhancing processing versatility to incorporate heat-sensitive ingredients.

ASSOCIATED CONTENT

Supporting Information (SI) is available free of charge on the ACS Publications website at DOI: xxx. See SI for supplementary Tables and Figure.

AUTHOR INFORMATION

Corresponding Author

* Fengwei Xie. Email: f.xie@uq.edu.au, fwhsieh@gmail.com

* Ling Chen. Email: felchen@scut.edu.cn

Author Contributions

The manuscript was written through contributions of all authors. All authors have given approval

to the final version of the manuscript.

Notes

The authors declare no competing financial interest.

ABBREVIATIONS

IL, ionic liquid; [C$_2$mim][OAc], 1-ethyl-3-methylimidazolium acetate; SEM, scanning electron

microscope; XRD, X-ray diffraction; ATR-FTIR, attenuated total reflectance-Fourier transform

infrared; SAXS, small-angle X-ray scattering; TGA, thermogravimetric analysis.

REFERENCES

1.   Laurent, A.; Olsen, S. I.; Hauschild, M. Z., Limitations of carbon footprint as indicator of environmental sustainability. *Environ. Sci. Technol.* **2012,** *46* (7), 4100-4108, DOI 10.1021/es204163f.

2.   Mekonnen, T.; Mussone, P.; Khalil, H.; Bressler, D., Progress in bio-based plastics and plasticizing modifications. *J. Mater. Chem. A* **2013,** *1* (43), 13379-13398, DOI 10.1039/C3TA12555F.

3.   Liu, H.; Xie, F.; Yu, L.; Chen, L.; Li, L., Thermal processing of starch-based polymers. *Prog. Polym. Sci.* **2009,** *34* (12), 1348-1368, DOI 10.1016/j.progpolymsci.2009.07.001.

4.   Turner, M. B.; Spear, S. K.; Holbrey, J. D.; Rogers, R. D., Production of bioactive cellulose films reconstituted from ionic liquids. *Biomacromolecules* **2004,** *5* (4), 1379-1384, DOI 10.1021/bm049748q.

5.   Turner, M. B.; Spear, S. K.; Holbrey, J. D.; Daly, D. T.; Rogers, R. D., Ionic liquid-reconstituted cellulose composites as solid support matrices for biocatalyst immobilization. *Biomacromolecules* **2005,** *6* (5), 2497-2502, DOI 10.1021/bm050199d.

6.   King, C.; Shamshina, J. L.; Gurau, G.; Berton, P.; Khan, N. F. A. F.; Rogers, R. D., A platform for more sustainable chitin films from an ionic liquid process. *Green Chem.* **2017,** *19* (1), 117-126, DOI 10.1039/C6GC02201D.

7.   Matet, M.; Heuzey, M.-C.; Pollet, E.; Ajji, A.; Avérous, L., Innovative thermoplastic chitosan obtained by thermo-mechanical mixing with polyol plasticizers. *Carbohydr. Polym.* **2013,** *95* (1), 241-251, DOI 10.1016/j.carbpol.2013.02.052.

8.   Xie, D. F.; Martino, V. P.; Sangwan, P.; Way, C.; Cash, G. A.; Pollet, E.; Dean, K. M.; Halley, P. J.; Avérous, L., Elaboration and properties of plasticised chitosan-based exfoliated nano-biocomposites. *Polymer* **2013,** *54* (14), 3654-3662, DOI 10.1016/j.polymer.2013.05.017.

9.   Li, M.; Liu, P.; Zou, W.; Yu, L.; Xie, F.; Pu, H.; Liu, H.; Chen, L., Extrusion processing and characterization of edible starch films with different amylose contents. *J. Food Eng.* **2011,** *106* (1), 95-101, DOI 10.1016/j.jfoodeng.2011.04.021.

10.   Xie, F.; Halley, P. J.; Avérous, L., Rheology to understand and optimize processibility, structures and properties of starch polymeric materials. *Prog. Polym. Sci.* **2012,** *37* (4), 595-623, DOI

10.1016/j.progpolymsci.2011.07.002.

11.   Xie, F.; Pollet, E.; Halley, P. J.; Avérous, L., Starch-based nano-biocomposites. *Prog. Polym. Sci.* **2013,** *38* (10-11), 1590-1628, DOI 10.1016/j.progpolymsci.2013.05.002.

12.   Pérez, S.; Baldwin, P. M.; Gallant, D. J., Structural features of starch granules I. In *Starch (Third Edition)*, James, B.; Roy, W., Eds. Academic Press: San Diego, 2009; pp 149-192, DOI 10.1016/B978-0-12-746275-2.00005-7.

13.   Jane, J.-l., Structural features of starch granules II. In *Starch (Third Edition)*, James, B.; Roy, W., Eds. Academic Press: San Diego, 2009; pp 193-236, DOI 10.1016/B978-0-12-746275-2.00006-9.

14.   Pérez, S.; Bertoft, E., The molecular structures of starch components and their contribution to the architecture of starch granules: a comprehensive review. *Starch/Stärke* **2010,** *62* (8), 389-420, DOI 10.1002/star.201000013.

15.   Fu, Z.-q.; Wang, L.-j.; Li, D.; Wei, Q.; Adhikari, B., Effects of high-pressure homogenization on the properties of starch-plasticizer dispersions and their films. *Carbohydr. Polym.* **2011,** *86* (1), 202-207, DOI 10.1016/j.carbpol.2011.04.032.

16.   Avérous, L., Biodegradable multiphase systems based on plasticized starch: a review. *Polym. Rev.* **2004,** *44* (3), 231-274, DOI 10.1081/MC-200029326.

17.   Campbell, M. R.; Yeager, H.; Abdubek, N.; Pollak, L. M.; Glover, D. V., Comparison of methods for amylose screening among amylose-extender (*ae*) maize starches from exotic backgrounds. *Cereal Chem.* **2002,** *79* (2), 317-321, DOI 10.1094/CCHEM.2002.79.2.317.

18.   Moran, J. I.; Cyras, V. P.; Giudicessi, S. L.; Erra-Balsells, R.; Vazquez, A., Influence of the Glycerol Content and Temperature on the Rheology of Native and Acetylated Starches During and After Gelatinization. *J. Appl. Polym. Sci.* **2011,** *120* (6), 3410-3420, DOI 10.1002/app.33347.

19.   Kurtzman, R. H.; Jones, F. T.; Bailey, G. F., Dissolution of starches in dimethylsulfoxide and variations in starches of several species, varieties, and maturities. *Cereal Chem.* **1973,** *50* (312), 312-322.

20.   Knutson, C. A.; Grove, M. J., Rapid method for estimation of amylose in maize starches. *Cereal Chem.* **1994,** *7* (5), 469-471.

21.   Hu, J. B.; Cheng, F.; Lin, Y.; Zhao, K.; Zhu, P. X., Dissolution of starch in urea/NaOH aqueous solutions. *J. Appl. Polym. Sci.* **2016,** *133* (19), DOI 10.1002/app.43390.

22.   Jordan, T.; Schmidt, S.; Liebert, T.; Heinze, T., Molten imidazole - a starch solvent. *Green Chem.* **2014,** *16* (4), 1967-1973, DOI 10.1039/c3gc41818a.

23.   Cowie, J. M. G., Studies on amylose and its derivatives. Part I. Molecular size and configuration of amylose molecules in various solvents. *Die Makromolekulare Chemie* **1960,** *42* (1), 230-247, DOI 10.1002/macp.1960.020420123.

24.   Aburto, J.; Alric, I.; Thiebaud, S.; Borredon, E.; Bikiaris, D.; Prinos, J.; Panayiotou, C., Synthesis, characterization, and biodegradability of fatty-acid esters of amylose and starch. *J. Appl. Polym. Sci.* **1999,** *74* (6), 1440-1451, DOI 10.1002/(SICI)1097-4628(19991107)74:6<1440::AID-APP17>3.0.CO;2-V.

25.   Fang, J. M.; Fowler, P. A.; Tomkinson, J.; Hill, C. A. S., The preparation and characterisation of a series of chemically modified potato starches. *Carbohydr. Polym.* **2002,** *47* (3), 245-252, DOI 10.1016/S0144-8617(01)00187-4.

26.   Heinze, T.; Talaba, P.; Heinze, U., Starch derivatives of high degree of functionalization. 1. Effective, homogeneous synthesis of p-toluenesulfonyl (tosyl) starch with a new functionalization pattern. *Carbohydr. Polym.* **2000,** *42* (4), 411-420, DOI 10.1016/S0144-8617(99)00182-4.

27.   Scott, M. P.; Brazel, C. S.; Benton, M. G.; Mays, J. W.; Holbrey, J. D.; Rogers, R. D., Application of ionic liquids as plasticizers for poly(methyl methacrylate). *Chem. Commun.* **2002,** (13), 1370-1371, DOI 10.1039/b204316p.

28.   Biswas, A.; Shogren, R. L.; Stevenson, D. G.; Willett, J. L.; Bhowmik, P. K., Ionic liquids as solvents for biopolymers: Acylation of starch and zein protein. *Carbohydr. Polym.* **2006,** *66* (4), 546-550, DOI 10.1016/j.carbpol.2006.04.005.

29.   Zhu, S.; Wu, Y.; Chen, Q.; Yu, Z.; Wang, C.; Jin, S.; Ding, Y.; Wu, G., Dissolution of cellulose with ionic liquids and its application: A mini-review. *Green Chem.* **2006,** *8* (4), 325-327, DOI 10.1039/B601395C.

30.   El Seoud, O. A.; Koschella, A.; Fidale, L. C.; Dorn, S.; Heinze, T., Applications of ionic liquids

in carbohydrate chemistry: A window of opportunities. *Biomacromolecules* **2007,** *8* (9), 2629-2647, DOI 10.1021/bm070062i.

31.   Zakrzewska, M. E.; Bogel-Łukasik, E.; Bogel-Łukasik, R., Solubility of carbohydrates in ionic liquids. *Energy Fuels* **2010,** *24* (2), 737-745, DOI 10.1021/ef901215m.

32.   Wilpiszewska, K.; Spychaj, T., Ionic liquids: Media for starch dissolution, plasticization and modification. *Carbohydr. Polym.* **2011,** *86* (2), 424-428, DOI 10.1016/j.carbpol.2011.06.001.

33.   Zhang, H.; Wu, J.; Zhang, J.; He, J., 1-Allyl-3-methylimidazolium chloride room temperature ionic liquid: A new and powerful nonderivatizing solvent for cellulose. *Macromolecules* **2005,** *38* (20), 8272-8277, DOI 10.1021/ma0505676.

34.   Heinze, T.; Schwikal, K.; Barthel, S., Ionic liquids as reaction medium in cellulose functionalization. *Macromol. Biosci.* **2005,** *5* (6), 520-525, DOI 10.1002/mabi.200500039.

35.   Qin, Y.; Lu, X.; Sun, N.; Rogers, R. D., Dissolution or extraction of crustacean shells using ionic liquids to obtain high molecular weight purified chitin and direct production of chitin films and fibers. *Green Chem.* **2010,** *12* (6), 968-971, DOI 10.1039/C003583A.

36.   Wu, Y.; Sasaki, T.; Irie, S.; Sakurai, K., A novel biomass-ionic liquid platform for the utilization of native chitin. *Polymer* **2008,** *49* (9), 2321-2327, DOI 10.1016/j.polymer.2008.03.027.

37.   Xie, H.; Zhang, S.; Li, S., Chitin and chitosan dissolved in ionic liquids as reversible sorbents of CO_2. *Green Chem.* **2006,** *8* (7), 630-633, DOI 10.1039/B517297G.

38.   Phillips, D. M.; Drummy, L. F.; Conrady, D. G.; Fox, D. M.; Naik, R. R.; Stone, M. O.; Trulove, P. C.; De Long, H. C.; Mantz, R. A., Dissolution and regeneration of bombyx mori silk fibroin using ionic liquids. *J. Am. Chem. Soc.* **2004,** *126* (44), 14350-14351, DOI 10.1021/ja046079f.

39.   Wang, Q.; Chen, Q.; Yang, Y.; Shao, Z., Effect of various dissolution systems on the molecular weight of regenerated silk fibroin. *Biomacromolecules* **2013,** *14* (1), 285-289, DOI 10.1021/bm301741q.

40.   Wang, Q.; Yang, Y.; Chen, X.; Shao, Z., Investigation of rheological properties and conformation of silk fibroin in the solution of AmimCl. *Biomacromolecules* **2012,** *13* (6), 1875-1881, DOI 10.1021/bm300387z.

41.   Pu, Y.; Jiang, N.; Ragauskas, A. J., Ionic liquid as a green solvent for lignin. *J. Wood Chem. Technol.* **2007,** *27* (1), 23-33, DOI 10.1080/02773810701282330.

42.   Xie, H.; Li, S.; Zhang, S., Ionic liquids as novel solvents for the dissolution and blending of wool keratin fibers. *Green Chem.* **2005,** *7* (8), 606-608, DOI 10.1039/B502547H.

43.   Wang, N.; Zhang, X.; Wang, X.; Liu, H., Ionic liquids modified montmorillonite/thermoplastic starch nanocomposites as ionic conducting biopolymer. *Macromol. Res.* **2009,** *17* (5), 285-288, DOI 10.1007/BF03218863.

44.   Wang, N.; Zhang, X.; Liu, H.; He, B., 1-Allyl-3-methylimidazolium chloride plasticized-corn starch as solid biopolymer electrolytes. *Carbohydr. Polym.* **2009,** *76* (3), 482-484, DOI 10.1016/j.carbpol.2008.11.005.

45.   Wang, N.; Zhang, X.; Liu, H.; Han, N., Ionically conducting polymers based on ionic liquid-plasticized starch containing lithium chloride. *Polym. Polym. Compos.* **2010,** *18* (1), 53-58.

46.   Ramesh, S.; Liew, C.-W.; Arof, A. K., Ion conducting corn starch biopolymer electrolytes doped with ionic liquid 1-butyl-3-methylimidazolium hexafluorophosphate. *J. Non-Cryst. Solids* **2011,** *357* (21), 3654-3660, DOI 10.1016/j.jnoncrysol.2011.06.030.

47.   Ramesh, S.; Shanti, R.; Morris, E.; Durairaj, R., Utilisation of corn starch in production of 'green' polymer electrolytes. *Mater. Res. Innovations* **2011,** *15* (1), s8, DOI 10.1179/143307511x13031890747291.

48.   Ramesh, S.; Shanti, R.; Morris, E., Studies on the thermal behavior of CS:LiTFSI:[Amim] Cl polymer electrolytes exerted by different [Amim] Cl content. *Solid State Sci.* **2012,** *14* (1), 182-186, DOI 10.1016/j.solidstatesciences.2011.11.022.

49.   Liew, C.-W.; Ramesh, S., Electrical, structural, thermal and electrochemical properties of corn starch-based biopolymer electrolytes. *Carbohydr. Polym.* **2015,** *124* (0), 222-228, DOI 10.1016/j.carbpol.2015.02.024.

50.   Liew, C.-W.; Ramesh, S.; Ramesh, K.; Arof, A. K., Preparation and characterization of lithium ion conducting ionic liquid-based biodegradable corn starch polymer electrolytes. *J. Solid State*

Electrochem. **2012,** *16* (5), 1869-1875, DOI 10.1007/s10008-012-1651-5.

51.   Wang, H.; Gurau, G.; Rogers, R. D., Ionic liquid processing of cellulose. *Chem. Soc. Rev.* **2012,** *41* (4), 1519-1537, DOI 10.1039/C2CS15311D.

52.   Sankri, A.; Arhaliass, A.; Dez, I.; Gaumont, A. C.; Grohens, Y.; Lourdin, D.; Pillin, I.; Rolland-Sabaté, A.; Leroy, E., Thermoplastic starch plasticized by an ionic liquid. *Carbohydr. Polym.* **2010,** *82* (2), 256-263, DOI DOI: 10.1016/j.carbpol.2010.04.032.

53.   Leroy, E.; Jacquet, P.; Coativy, G.; Reguerre, A. l.; Lourdin, D., Compatibilization of starch–zein melt processed blends by an ionic liquid used as plasticizer. *Carbohydr. Polym.* **2012,** *89* (3), 955-963, DOI 10.1016/j.carbpol.2012.04.044.

54.   Xie, F.; Flanagan, B. M.; Li, M.; Sangwan, P.; Truss, R. W.; Halley, P. J.; Strounina, E. V.; Whittaker, A. K.; Gidley, M. J.; Dean, K. M.; Shamshina, J. L.; Rogers, R. D.; McNally, T., Characteristics of starch-based films plasticised by glycerol and by the ionic liquid 1-ethyl-3-methylimidazolium acetate: a comparative study. *Carbohydr. Polym.* **2014,** *111*, 841-848, DOI 10.1016/j.carbpol.2014.05.058.

55.   Tan, I.; Flanagan, B. M.; Halley, P. J.; Whittaker, A. K.; Gidley, M. J., A method for estimating the nature and relative proportions of amorphous, single, and double-helical components in starch granules by ^{13}C CP/MAS NMR. *Biomacromolecules* **2007,** *8* (3), 885-891, DOI 10.1021/bm060988a.

56.   Mateyawa, S.; Xie, D. F.; Truss, R. W.; Halley, P. J.; Nicholson, T. M.; Shamshina, J. L.; Rogers, R. D.; Boehm, M. W.; McNally, T., Effect of the ionic liquid 1-ethyl-3-methylimidazolium acetate on the phase transition of starch: Dissolution or gelatinization? *Carbohydr. Polym.* **2013,** *94* (1), 520-530, DOI 10.1016/j.carbpol.2013.01.024.

57.   Young, J. F., Humidity control in the laboratory using salt solutions—a review. *Journal of Applied Chemistry* **1967,** *17* (9), 241-245, DOI 10.1002/jctb.5010170901.

58.   Lopez-Rubio, A.; Flanagan, B. M.; Gilbert, E. P.; Gidley, M. J., A novel approach for calculating starch crystallinity and its correlation with double helix content: A combined XRD and NMR study. *Biopolymers* **2008,** *89* (9), 761-768, DOI 10.1002/bip.21005.

59.   van Soest, J. J. G.; Hulleman, S. H. D.; de Wit, D.; Vliegenthart, J. F. G., Crystallinity in starch bioplastics. *Ind. Crops Prod.* **1996,** *5* (1), 11-22, DOI 10.1016/0926-6690(95)00048-8.

60.   Zhang, B.; Chen, L.; Li, X.; Li, L.; Zhang, H., Understanding the multi-scale structure and functional properties of starch modulated by glow-plasma: A structure-functionality relationship. *Food Hydrocolloids* **2015,** *50,* 228-236, DOI 10.1016/j.foodhyd.2015.05.002.

61.   Zhang, B.; Zhao, Y.; Li, X.; Li, L.; Xie, F.; Chen, L., Supramolecular structural changes of waxy and high-amylose cornstarches heated in abundant water. *Food Hydrocolloids* **2014,** *35,* 700-709, DOI 10.1016/j.foodhyd.2013.08.028.

62.   Zhang, B.; Chen, L.; Xie, F.; Li, X.; Truss, R. W.; Halley, P. J.; Shamshina, J. L.; Rogers, R. D.; McNally, T., Understanding the structural disorganization of starch in water-ionic liquid solutions. *Phys. Chem. Chem. Phys.* **2015,** *17,* 13860-13871, DOI 10.1039/c5cp01176k.

63.   Shi, W.; Damodaran, K.; Nulwala, H. B.; Luebke, D. R., Theoretical and experimental studies of water interaction in acetate based ionic liquids. *Phys. Chem. Chem. Phys.* **2012,** *14* (45), 15897-15908, DOI 10.1039/C2CP42975F.

64.   Xie, F.; Flanagan, B. M.; Li, M.; Truss, R. W.; Halley, P. J.; Gidley, M. J.; McNally, T.; Shamshina, J. L.; Rogers, R. D., Characteristics of starch-based films with different amylose contents plasticised by 1-ethyl-3-methylimidazolium acetate. *Carbohydr. Polym.* **2015,** *122,* 160-168, DOI 10.1016/j.carbpol.2014.12.072.

65.   Derek, R.; Prentice, M.; Stark, J. R.; Gidley, M. J., Granule residues and "ghosts" remaining after heating A-type barley-starch granules in water. *Carbohydr. Res.* **1992,** *227,* 121-130, DOI 10.1016/0008-6215(92)85065-8.

66.   Debet, M. R.; Gidley, M. J., Why do gelatinized starch granules not dissolve completely? Roles for amylose, protein, and lipid in granule "ghost" integrity. *J. Agric. Food Chem.* **2007,** *55* (12), 4752-4760, DOI 10.1021/jf070004o.

67.   Buléon, A.; Colonna, P.; Planchot, V.; Ball, S., Starch granules: structure and biosynthesis. *Int. J. Biol. Macromol.* **1998,** *23* (2), 85-112, DOI 10.1016/S0141-8130(98)00040-3.

68.   Zhang, B.; Zhao, Y.; Li, X.; Zhang, P.; Li, L.; Xie, F.; Chen, L., Effects of amylose and phosphate monoester on aggregation structures of heat-moisture treated potato starches. *Carbohydr. Polym.* **2014,** *103*, 228-233, DOI 10.1016/j.carbpol.2013.12.055.

69.   Cheetham, N. W. H.; Tao, L., Variation in crystalline type with amylose content in maize starch granules: an X-ray powder diffraction study. *Carbohydr. Polym.* **1998,** *36* (4), 277-284, DOI Doi: 10.1016/s0144-8617(98)00007-1.

70.   Lopez-Rubio, A.; Flanagan, B. M.; Shrestha, A. K.; Gidley, M. J.; Gilbert, E. P., Molecular rearrangement of starch during in vitro digestion: toward a better understanding of enzyme resistant starch formation in processed starches. *Biomacromolecules* **2008,** *9* (7), 1951-8, DOI 10.1021/bm800213h.

71.   Zhang, B.; Chen, L.; Xie, F.; Li, X.; Truss, R. W.; Halley, P. J.; Shamshina, J. L.; Rogers, R. D.; McNally, T., Understanding the structural disorganization of starch in water-ionic liquid solutions. *Phys. Chem. Chem. Phys.* **2015,** *17* (21), 13860-13871, DOI 10.1039/C5CP01176K.

72.   Beaucage, G., Determination of branch fraction and minimum dimension of mass-fractal aggregates. *Phys. Rev. E: Stat., Nonlinear, Soft Matter Phys.* **2004,** *70* (3), 031401, DOI 10.1103/PhysRevE.70.031401.

73.   Lopez-Rubio, A.; Htoon, A.; Gilbert, E. P., Influence of extrusion and digestion on the nanostructure of high-amylose maize starch. *Biomacromolecules* **2007,** *8* (5), 1564-1572, DOI 10.1021/bm061124s.

74.   Daniels, D. R.; Donald, A. M., Soft material characterization of the lamellar properties of starch: Smectic side-chain liquid-crystalline polymeric approach. *Macromolecules* **2004,** *37* (4), 1312-1318, DOI 10.1021/ma030360h.

75.   Vermeylen, R.; Derycke, V.; Delcour, J. A.; Goderis, B.; Reynaers, H.; Koch, M. H. J., Gelatinization of starch in excess water: Beyond the melting of lamellar crystallites. A combined wide- and small-angle X-ray scattering study. *Biomacromolecules* **2006,** *7* (9), 2624-2630, DOI 10.1021/bm060252d.

76.   Li, M.; Xie, F.; Hasjim, J.; Witt, T.; Halley, P. J.; Gilbert, R. G., Establishing whether the

structural feature controlling the mechanical properties of starch films is molecular or crystalline. *Carbohydr. Polym.* **2015,** *117*, 262-270, DOI 10.1016/j.carbpol.2014.09.036.

77.   Xie, F.; Flanagan, B. M.; Li, M.; Truss, R. W.; Halley, P. J.; Gidley, M. J.; McNally, T.; Shamshina, J. L.; Rogers, R. D., Characteristics of starch-based films with different amylose plasticised by 1-ethyl-3-methylimidazolium acetate contents. *Carbohydr. Polym.* **2015,** *122*, 160-168, DOI 10.1016/j.carbpol.2014.12.072.

78.   Zhang, B.; Xie, F.; Zhang, T.; Chen, L.; Li, X.; Truss, R. W.; Halley, P. J.; Shamshina, J. L.; McNally, T.; Rogers, R. D., Different characteristic effects of ageing on starch-based films plasticised by 1-ethyl-3-methylimidazolium acetate and by glycerol. *Carbohydr. Polym.* **2016,** *146*, 67-79, DOI 10.1016/j.carbpol.2016.03.056.

79.   Wendler, F.; Todi, L.-N.; Meister, F., Thermostability of imidazolium ionic liquids as direct solvents for cellulose. *Thermochim. Acta* **2012,** *528* (0), 76-84, DOI 10.1016/j.tca.2011.11.015.

80.   Liu, X.; Yu, L.; Liu, H.; Chen, L.; Li, L., Thermal decomposition of corn starch with different amylose/amylopectin ratios in open and sealed systems. *Cereal Chem.* **2009,** *86* (4), 383-385, DOI doi:10.1094/CCHEM-86-4-0383.

81.   Liu, X.; Yu, L.; Xie, F.; Li, M.; Chen, L.; Li, X., Kinetics and mechanism of thermal decomposition of cornstarches with different amylose/amylopectin ratios. *Starch/Stärke* **2010,** *62* (3-4), 139-146, DOI 10.1002/star.200900202.

- Table of Contents -

Facile preparation of starch-based electroconductive films with ionic liquid

Binjia Zhang [a,b,c], *Fengwei Xie* [*c], *Julia L. Shamshina* [d,e], *Robin D. Rogers* [e], *Tony McNally* [f],

David K. Wang [g], *Peter J. Halley* [c], *Rowan W. Truss* [c], *Siming Zhao* [b], *Ling Chen* [*a]
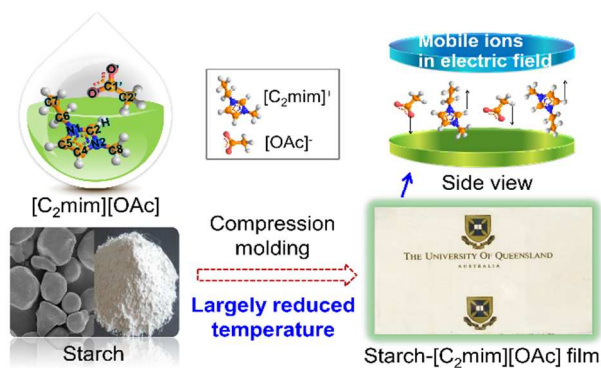
With an ionic liquid (1-ethyl-3-methylimidazolium acetate, [C$_2$mim][OAc]), starch was facilely

processed into optically-transparent electroconductive films at greatly reduced temperature,

relative to that commonly used in biopolymer melt processing.